

Supporting Material for

Conformational states of melittin at a bilayer interface

Magnus Andersson,^{*}¶ Jakob P. Ulmschneider,[†] Martin B. Ulmschneider,[‡] and Stephen H. White^{*}

^{*} Department of Physiology and Biophysics, University of California, Irvine, USA; [†]Institute of Natural Sciences, Shanghai Jiao Tong University, 800 Dongchuan Road, Shanghai, 200240 Shanghai, China; [‡]Department of Crystallography, Institute of Structural and Molecular Biology, Birkbeck College, University of London, Malet Street, London WC1E 7HX, U.K.;

[¶]Present address: Science for Life Laboratory, Department of Biochemistry and Biophysics, Stockholm University, SE-106 91 Stockholm, Sweden

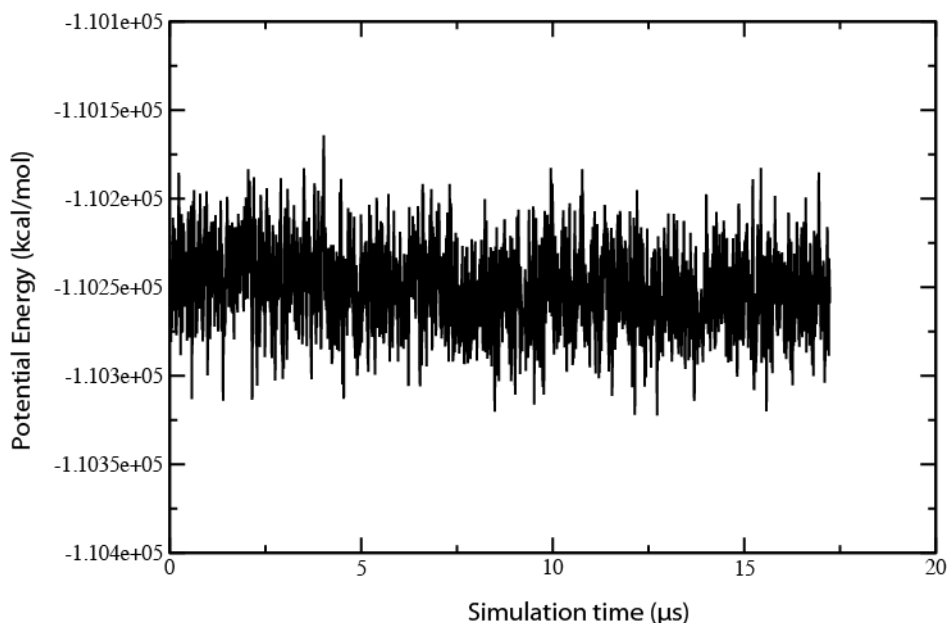


Figure S1. Energetic stability of the CHARMM simulation system in the isothermic-isobaric (NPT) ensemble. The potential energy (kcal/mol) includes the bonded and non-bonded terms for the entire system (2 melittin peptides, 264 DOPC lipids, 10,686 water molecules, and 24 Cl^- ions).

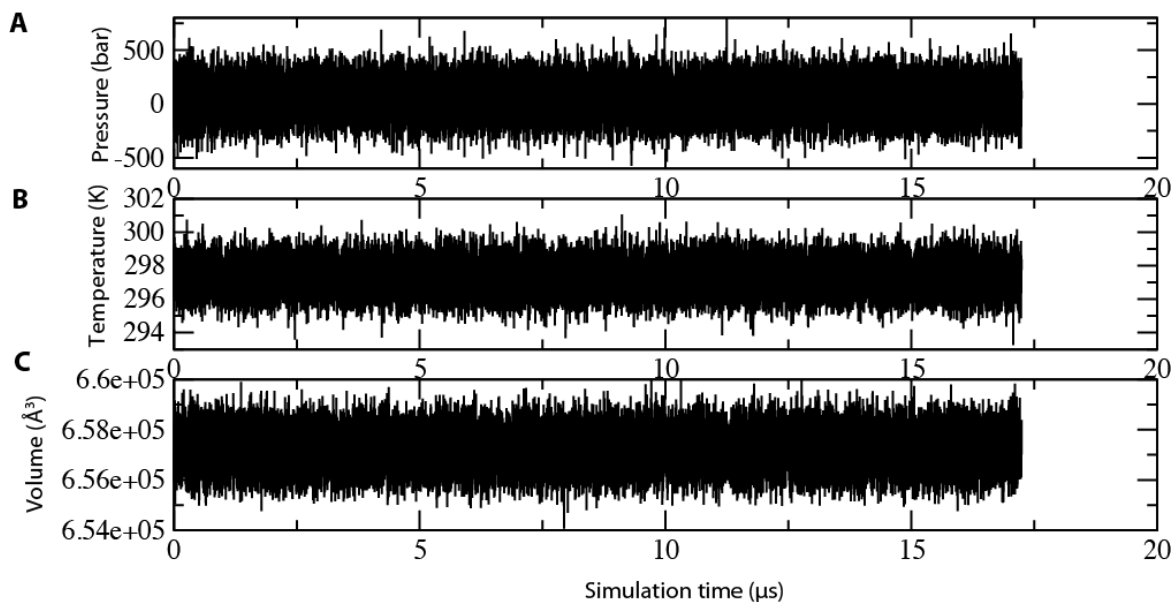


Figure S2. Stability of Berendsen baro- and thermostats, and volume variation of the simulation cell in the CHARMM simulation system. The evolution of (A) pressure (bar) and (B) temperature (K) show that the simulation system was devoid of any cold/hot spots, which can lead to problems by numerical overflow. (C) The evolution of the simulation box volume (\AA^3) further demonstrates the stability of the system.

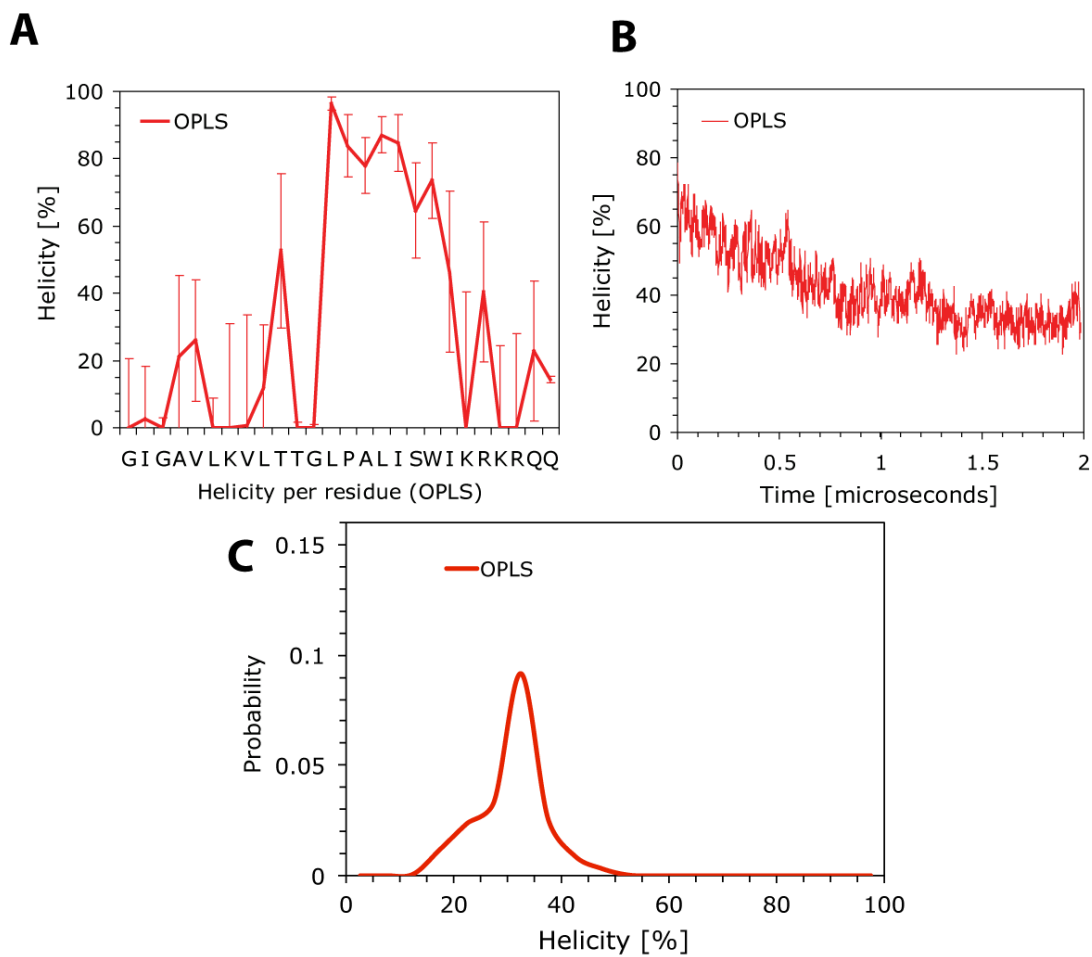
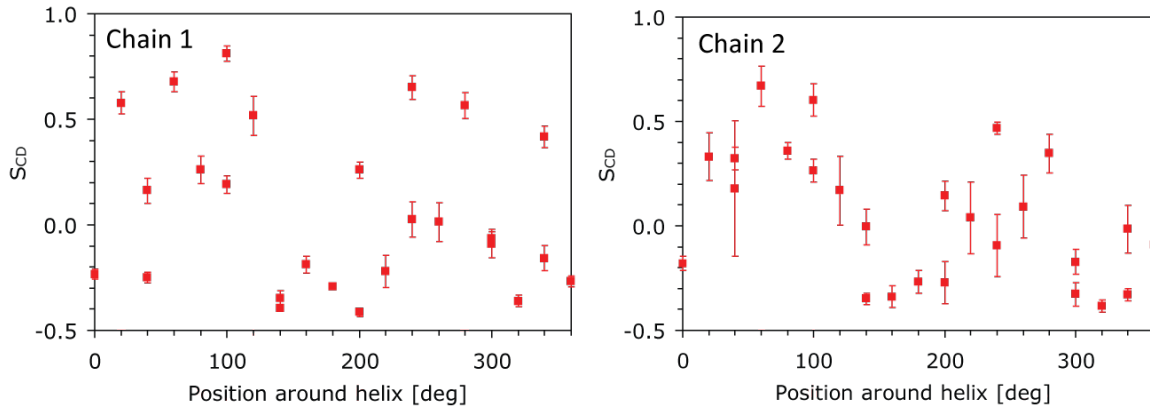


Figure S3. Helicity and conformational distribution of melittin as determined via MD simulation using the OPLS forcefield. The helicity per residue for MLT1 and MLT2 are reported in (A) and the corresponding evolution of the helicity are shown in (B). The conformational distributions over the entire 17 μ s simulation are shown in (C).



Position [deg]	residue	S_{CD} (chain 1)	S_{CD} (chain 2)
0	GLY-1	-0.234	-0.179
100	ILE-2	0.191	0.263
200	GLY-3	0.259	0.144
300	ALA-4	-0.064	-0.172
40	VAL-5	0.162	0.323
140	LEU-6	-0.394	-0.348
240	LYS-7	0.651	0.467
340	VAL-8	0.417	-0.330
80	LEU-9	0.261	0.359
180	THR-10	-0.292	-0.268
280	THR-11	0.565	0.347
20	GLY-12	0.577	0.332
120	LEU-13	0.517	0.169
220	PRO-14	-0.222	0.039
320	ALA-15	-0.361	-0.385
60	LEU-16	0.678	0.669
160	ILE-17	-0.189	-0.339
260	SER-18	0.013	0.091
360	TRP-19	-0.269	-0.089
100	ILE-20	0.811	0.602
200	LYS-21	-0.415	-0.272
300	ARG-22	-0.089	-0.328
40	LYS-23	-0.250	0.179
140	ARG-24	-0.346	-0.005
240	GLN-25	0.027	-0.094
340	GLN-26	-0.158	-0.016

Figure S4. S_{CD} order parameter $S_{CD} = \langle (1/2)(3\cos^2 q - 1) \rangle$ for the angle θ between the $C_\alpha - C_\beta$ bond and the z-axis, for each residue, averaged over the 17 μ s MD simulation using the CHARMM force field. Due to the one transition at 8 μ s, the errors (from block averaging) in chain 2 are larger than for chain 1.

Methods

The CHARMM approach

Building the system

The initial simulation system configuration was derived from the end of previous 12 ns simulation (1), which contained four melittin peptides (PDB ID 2MLT) partitioned into a 264-lipid DOPC bilayer. We removed one melittin peptide from each leaflet and solvated the system with 10,686 water molecules and added 24 Cl⁻ counterions to achieve electrical neutrality.

Molecular dynamics simulation

The μ s-timescale simulations were performed on Anton, a special-purpose computer for molecular dynamics simulations of biomolecules (2). The system was equilibrated for 10 ns using the Desmond Molecular Dynamics System, version 2.4 (D. E. Shaw Research, New York, NY, 2008) on a conventional high performance cluster before being transferred to Anton. The CHARMM22 (3) and CHARMM36 (4) force fields were used for the protein and lipids, respectively, and the TIP3P model was used for water. A reversible multiple-timestep algorithm was employed to integrate the equations of motion with a time step of 6 fs for the long-range non-bonded forces, and 2 fs for short-range non-bonded and bonded forces. All bond lengths involving hydrogen atoms were held fixed using the SHAKE algorithm. The k-space Gaussian split Ewald method (5) with a 32 x 32 x 32 grid was used to calculate long-range electrostatic interactions. A cutoff of 14 Å was used for the Lennard-Jones and short-range electrostatic interactions. The simulations were performed at constant temperature (300 K) and pressure (1 atm), using a Berendsen thermostat and semi-isotropic Berendsen barostat. Analyses and visualization were performed with VMD 1.9 (6).

The OPLS approach

One melittin peptide was embedded into the water phase of a box containing a preformed DOPC lipid bilayers made up of 72 lipids. The initial conformation was an ideal α -helix, placed 10 Å from the bilayer surface. The simulation was performed and analyzed using Gromacs version 4.0 (www.gromacs.org) (7) and hippo beta (www.biowerkzeug.com), using OPLS-AA for the protein (8), TIP3P for water (9), and united atom lipid parameters for DOPC (10). Electrostatic interactions were computed using Ewald-based PME, and a cutoff of 10 Å was used for van der Waals interactions. Bonds involving hydrogen atoms were restrained using LINCS (11). Simulations were run with a 2 fs integration time-step and neighbor lists were updated every 5 steps. All simulations are performed in the NPT ensemble, with no additional applied surface tension. Water, lipids, and the protein were each coupled separately to a v-rescale thermostat, which is a Berendsen thermostat with occasional randomizing of the velocities, with time constant $\tau_T = 0.1$ ps using weak temperature coupling (12). Atmospheric pressure of 1 bar was maintained using weak

semi-isotropic Berendsen pressure coupling with compressibility $\kappa_z = \kappa_{xy} = 4.6 \cdot 10^{-5} \text{ bar}^{-1}$ and time constant $\tau_p = 1 \text{ ps}$ (13). 2.0 μs of MD was run at 300 K.

Supporting References

1. Benz, R. W., H. Nanda, *et al.* 2006. Diffraction-based density restraints for membrane and membrane/protein molecular dynamics simulations. *Biophys. J.* 91:3617-3629.
2. Shaw, D. E., M. M. Deneroff, *et al.* 2007. Anton, a special-purpose machine for molecular dynamics simulation. *Proc. 34th Annu. Internat. Sym. Computer Architect.*
3. MacKerell, A. D., Jr., M. Feig, and C. L. Brooks, II. 2004. Extending the treatment of backbone energetics in protein force fields: Limitations of gas-phase quantum mechanics in reproducing conformational distributions in molecular dynamics simulations. *J. Comput. Chem.* 25:1400-1415.
4. Klauda, J. B., R. M. Venable, *et al.* 2010. Update of the CHARMM all-atom additive force field for lipids: validation on six lipid types. *J. Phys. Chem. B* 114:7830-7843.
5. Shan, Y., J. L. Klepeis, *et al.* 2005. Gaussian split Ewald: a fast Ewald mesh method for molecular simulation. *J. Chem. Phys.* 122:054101-054101 to 054101-054113.
6. Humphrey, W., W. Dalke, and K. Schulten. 1996. VMD: Visual molecular dynamics. *J. Mol. Graph.* 14:33-38.
7. Berendsen, H. J. C., D. van der Spoel, and R. van Drunen. 1995. GROMACS: A new message-passing parallel molecular dynamics implementation. *Comput. Phys. Commun.* 91:43-56.
8. Jorgensen, W. L., D. S. Maxwell, and J. Tirado-Rives. 1996. Development and testing of the OPLS all-atom force field on conformational energetics and properties of organic liquids. *J. Am. Chem. Soc.* 118:11225-11236.
9. Jorgensen, W. L., J. Chandrasekhar, *et al.* 1983. Comparison of simple potential functions for simulating liquid water. *J. Chem. Phys.* 79:926-935.
10. Ulmschneider, J. P., and M. B. Ulmschneider. 2009. United atom lipid parameters for combination with the optimized potentials for liquid simulations all-atom force fields. *J. Chem. Theor. Comput.* 5:1803-1813.
11. Hess, B., H. Bekker, *et al.* 1997. LINCS: A linear constraint solver for molecular simulations. *J. Comput. Biol.* 18:1463-1472.
12. Bussi, G., D. Donadio, and M. Parrinello. 2007. Canonical sampling through velocity rescaling. *J. Chem. Phys.* 126:014101.
13. Berendsen, H. J. C., J. P. M. Postma, *et al.* 1984. Molecular-dynamics with coupling to an external bath. *J. Chem. Phys.* 81:3684-3690.